Optical Properties of Emeraldine Salt Polymers from Ab Initio Calculations: Comparison with Recent Experimental Data

Renato Colle,*,† Pietro Parruccini,† Andrea Benassi,‡,§ and Carlo Cavazzoni†,||

Dipartimento di Chimica Applicata e Scienza dei Materiali, Universitá di Bologna, via Saragozza, 8 I-40136 Bologna, Italy, INFM-National Research Center on nanoStructures and bioSystems at Surfaces (S3), Dipartimento di Fisica, Universitá di Modena e Reggio Emilia, Via Campi 213/A, I-41100 Modena, Italy, and High Performance Computing Department CINECA, I-40136 Bologna, Italy

Received: November 27, 2006; In Final Form: January 17, 2007

We present the absorption coefficient $\alpha(\omega)$, the transverse dielectric function $\epsilon(\omega)$, the optical conductivity $\sigma(\omega)$, and the reflectance $R(\omega)$ calculated for an emeraldine salt conducting polymer in its crystalline 3D polaronic structure. We utilize Kohn−Sham density functional theory (DFT) electronic wavefunctions and energies implemented in the expression of the macroscopic transverse dielectric function in the framework of the band theory without the electron−hole interaction. Contributions of intra-band transitions are taken into account by adding a Drude-like term to the dielectric function calculated ab initio. Comparison with optical properties, recently measured on high-quality emeraldine salts (Lee, K.; Cho, S.; Park, S. H.; Heeger, A. J.; Lee, C.-W.; Lee, S. H. *Nature* **2006**, *441*, 65), and with optical absorption spectra, recorded on other emeraldine salts, is very satisfactory. The calculated spectra are discussed in terms of energy-band structure, density of states, inter- and intra-band transitions, and transverse dielectric function.

1. Introduction

Conducting polymers are a new[1−3] and exciting field of research at the boundary between chemistry and condensed matter physics. They address a number of theoretical questions of enormous interest[4,5] and open the possibility of several important technological applications.[6−13]

Conducting polymers are conjugated systems in which the electronic delocalization, due to π-bonding, provides conditions for charge mobility along the backbone of the polymer chains. Furthermore, the electron attraction with the nuclei of the neighboring chains also makes interchain electron transfer possible, favored by the crystalline order of the structure. The conducting properties of these polymers depend on the characteristics of their repeat unit and can be reversibly modified from insulator to metal by introducing p-type or n-type carriers via electrochemical doping[12,14] or acid−base chemistry (protonation).[15−18]

Among conducting polymers, polyanilines (PANI)[19] have given the first example of a conjugated polymer converted by the solvent (a protonic acid) from a semiconductor form (emeraldine base EB) to a conducting form (emeraldine salt ES), which can be processed directly into the metallic salt from the concentrated acid solution.[20] The solubility of the resulting PANI complex in common organic solvents[21] has opened the way to processing the conducting polymer with other commercial polymers into films and polymer blends.[22] The existence of phase segregation into metallic and nonmetallic phases[18,23] and of crystalline and amorphous regions in the ES powders and films has been evidenced by various experimental studies,[23−29] together with the existence of two classes (ES-I and ES-II) of the conducting polymer[24−26] obtained from acidification of EB by HCl.

In a single chain representation of the polymer structure, the repeat unit of EB is $[(1A)(2A)]_n$, with (1A) ≡ (B−NH−B−NH−) and (2A) ≡ (B−N═Q═N−), B and Q being a benzenoid and a quinoid ring, respectively. Protonation of this unit produces a structural change of the chain, without changing however the number of electrons,[30,31] and leads to emeraldine salts with a chain repeat unit: $[(1S)^{\bullet+}(C)^-]_n$, where $(1S)^{\bullet+} \equiv (B-NH-B-NH-)^{\bullet+}$ and $(C)^-$ is the counterion (e.g., Cl^-, ClO_4^-, HSO_4^-, CS^-, ...) . The repeat unit $[(1S)^{\bullet+}]_n$ has an unpaired electron in a half-filled band, which leads to a metallic state described as a polaronic metal.[32]

The characterization of the emeraldine salts as conducting polymers has been extensively performed by probing their electronic structure through optical studies (mainly absorption spectra and photoinduced absorption spectra) of films cast from acid solutions[18,20,32] and of the polymer dissolved in acid solutions.[20,33] The experimental spectra have been interpreted utilizing VEH band-structure calculations[34,35] performed on a single-chain model of the polymer, without calculating, however, dielectric function and related optical properties. The VEH technique has been also used to characterize chain geometry and electronic modifications induced in isolated PANI chains by doping.[36] More recently, DFT calculations have been performed[37] to compare structural properties and relative energies of isolated EB and ES polymer chains involved in the mechanism of HCl/EB protonation. In a recent paper,[49] the HCl protonation process of the EB-II polymer to give the ES-II

* E-mail: colle@sns.it (R.C.).
† Dipartimento di Chimica Applicata e Scienza dei Materiali.
‡ INFM-National Research Center on nanoStructures and bioSystems at Surfaces (S3).
§ Dipartimento di Fisica.
|| High Performance Computing Department CINECA.

10.1021/jp067847n CCC: $37.00
Published on Web 03/01/2007

crystalline salt has been simulated using Car−Parrinello molecular dynamics.[50,51] We have shown that a *Pc2a* lattice structure of polymer chains, drastically rearranged with respect to those of EB-II[52] and with chlorine ions distributed in polaronic arrangement, is in good agreement with the available X-ray experimental data[24,25] recorded on ES-II polymers.

Optical, magnetic, and transport properties of polyanilines in their metallic state have been intensively studied in the past decade.[38−46] The measured low-frequency dependence of the optical conductivity $\sigma(\omega)$ and of the real part of the dielectric function $\epsilon_1(\omega)$, and the low temperature behavior of the resistivity, have been found to be not those expected for conventional metals. A few months ago, truly metallic polymers characterized by classic metallic transport data were eventually obtained[47] from samples of PANI-EB prepared with the self-stabilized dispersion polymerization (SSDP) technique[48] and doped with camphor sulfonic acid (CSA) to give PANI-CSA salts. Measures of resistivity, down to $T \sim 5$ K, and of $\sigma(\omega)$, $\epsilon_1(\omega)$, and reflectance $R(\omega)$ below 2000 cm^{-1} have confirmed the true metallic character of protonated PANI when prepared from high-quality unprotonated PANI-EB samples with a low density of structural defects. This decisive step in the characterization of ES polymers as true metallic systems shows the importance of an ordered structure of regular chains. This fact also makes the theoreticians more confident in modeling the crystalline regions of such systems as 3D perfect crystals of mutually interacting[46] regular chains, a model that is particularly suitable for ab initio calculations of the electronic and optical properties that characterize the "metallic state" of these polymers.

In this paper, we calculate the absorption coefficient $\alpha(\omega)$, the complex dielectric function $\epsilon(\omega)$, the optical conductivity $\sigma(\omega)$, and the reflectance $R(\omega)$ of a 3D crystal of ES-II polymer in its polaronic structure.[49] We utilize Kohn−Sham DFT electronic wavefunctions and energies implemented in the expression of the macroscopic transverse dielectric function in the framework of the band theory without the electron−hole interaction.[53] In this calculation, we have included only vertical band-to-band transitions. To also take into account contributions of the intra-band transitions, we have added, to the dielectric function calculated ab initio, a Drude-like term appropriate for metallic systems. The resulting global expression of $\epsilon(\omega)$ allows us to reproduce quite satisfactorily the measured ω-dependence of the main optical properties in the range of frequencies from ~0.2 to above 4 eV.

We point out that several first-principles calculations of electronic and optical properties of crystalline conjugated polymers[54] and oligomers[55,56] have been performed also using correlated many-body techniques. To our knowledge, however, this is the first attempt to construct, from ab initio calculations, optical spectra of a crystalline conducting polymer obtained by chemical doping of a conjugated polymer.

In Section 2, we present the quantum-mechanical expressions used for calculating the optical quantities of interest, and we describe the computational procedures used for their evaluation. In Section 3.1, we present the optical absorption spectrum calculated for a 3D crystal of ES-II[49] in its polaronic structure obtained from HCl protonation of EB-II,[52] and we discuss the absorption spectrum in terms of band structure and density of states resulting from KS-DFT calculations. We also compare the optical absorption spectrum calculated for ES-II with that calculated for the EB-II polymer[52] and with experimental spectra recorded on solid samples of the two polymers.[18,20,32] Finally, in Section 3.2, we calculate the optical spectra of the real part of the dielectric function, optical conductivity, and reflectance of ES-II, identifying the spectral contributions due to the inter- and intra-band electronic transitions. The calculated spectra are compared with those recently measured on PANI-CSA salts.[47] Conclusions are drawn in Section 4.

2. Method

We have carried out KS-DFT calculations of energy-band structure, density of states, and electronic wavefunctions of a perfect 3D crystal of ES-II in its polaronic structure with lattice parameters and chain geometry taken from ref 49. To this end, we have used the package of programs Quantum-Espresso,[57] which performs ab initio calculations of ground-state energy, energy gradient, electronic wavefunctions, and properties of periodic systems. These codes use plane-wave expansions for the single particle wavefunctions, pseudopotentials (ECP) for the core electrons, and various energy functionals for the exchange-correlation potential. In our KS-DFT calculations, we have used a kinetic energy cutoff of 70 Ry, different grids of *k*-points up to a maximum of 2200 points, the norm-conserving ECP of Martin and Troullier,[58] and the Becke−Lee−Yang−Parr (BLYP) exchange-correlation functional.[59,60] Energy bands and wavefunctions obtained from these calculations have been used for evaluating the macroscopic transverse dielectric function, whose real and imaginary parts enter into the definition of the main optical properties of a condensed system.

For an incident light of frequency ω, wave vector $\vec{q}$, and polarization direction $\hat{e}$, the macroscopic transverse dielectric function, defined in the framework of the band theory without the electron−hole interaction, is given by

$$\epsilon(\vec{q},\hat{e};\omega) = 1 + \frac{4\pi\hbar^2e^2}{m^2V}\sum_{c\vec{k}_c}\sum_{v\vec{k}_v}\frac{(n_{v\vec{k}_v} - n_{c\vec{k}_c})\ |\langle\Psi_{c\vec{k}_c}|e^{i\vec{q}\cdot\vec{r}}\hat{e}\cdot\vec{p}|\Psi_{v\vec{k}_v}\rangle|^2}{(E_{c\vec{k}_c} - E_{v\vec{k}_v})^2(E_{c\vec{k}_c} - E_{v\vec{k}_v} - \hbar\omega - i\eta)} \quad (1)$$

with $\eta \rightarrow 0^+$. In eq 1, $\{\Psi_{j\vec{k}_j}(\vec{r})\}$ are crystalline orbitals of energy $E_{j\vec{k}_j}$ and of occupation number $n_{j\vec{k}_j}$, and V is the crystalline volume given by the product of the cell volume times the number of cells.

In dipole approximation ($q = 0$) and expanding the crystalline orbitals in terms of plane waves of the reciprocal lattice for each $\vec{k}$ of the first Brillouin zone, $\Psi_{j\vec{k}}(\vec{r}) = (1/\sqrt{V})\sum_{\vec{g}\in RL}C_j(\vec{k}+\vec{g})e^{i(\vec{k}+\vec{g})\cdot\vec{r}}$, the transition matrix element in eq 1 becomes

$$\langle\Psi_{c\vec{k}_c}|\hat{e}\cdot\vec{p}|\Psi_{v\vec{k}_v}\rangle = \hbar\delta_{\vec{k}_c,\vec{k}_v}\sum_{\vec{g}\in RL}\hat{e}\cdot(\vec{k}_v+\vec{g})C_c^*(\vec{k}_c+\vec{g})C_v(\vec{k}_v+\vec{g}) = M_{c,v}(\hat{e},\vec{k}); \qquad \vec{k} = \vec{k}_c = \vec{k}_v \quad (2)$$

Note that, in our calculations, the core electrons are not included explicitly, but only through ECP; thus the crystalline orbitals, obtained from the solution of the KS-equations, are "pseudo" wavefunctions, which overlap the "exact" ones only beyond the "core radius" of the various atoms. The corrections to the dipole matrix elements due to the ECP nonlocal terms in the Hamiltonian have been neglected in our calculations, together with local field effects due to the inhomogeneity of the crystal.[61]

Taking the limit of small, but nonvanishing η in eq 1, a procedure that accounts for the non-monochromaticity of the incident light and the finite lifetime of the excited levels, we

obtain the following Drude−Lorentz expression for the dielectric function:

$$\epsilon(\hat{e};\omega) = 1 + \omega_p^2 \sum_{c,v} \sum_{\vec{k}} \frac{f_{v\vec{k}}^{c\vec{k}}(\hat{e})}{[(\omega_{c\vec{k}} - \omega_{v\vec{k}})^2 - \omega^2] - i\Gamma\omega} \quad (3)$$

where $\omega_{c\vec{k}} = E_{c\vec{k}}/\hbar$ and $\Gamma = 2\eta/\hbar$. Furthermore, $\omega_p = \sqrt{(4\pi e^2/m)N}$ is the free-electron plasma frequency with N being the number of electrons per unit volume; $f_{v\vec{k}}^{c\vec{k}}(\hat{e})$ is the oscillator strength of the $|\Psi_{v\vec{k}_v}\rangle \rightarrow |\Psi_{c\vec{k}_c}\rangle$ transition:

$$f_{v\vec{k}}^{c\vec{k}}(\hat{e}) = \frac{2n_{v\vec{k}}}{\hbar m N V} \frac{|M_{c,v}(\hat{e},\vec{k})|^2}{\omega_{c\vec{k}} - \omega_{v\vec{k}}} \quad (4)$$

The real and imaginary parts of $\epsilon(\hat{e};\omega)$ are, respectively,

$$\epsilon_1(\hat{e};\omega) = 1 + \omega_p^2 \sum_{c,v} \sum_{\vec{k}} f_{v\vec{k}}^{c\vec{k}}(\hat{e}) \frac{[(\omega_{c\vec{k}} - \omega_{v\vec{k}})^2 - \omega^2]}{[(\omega_{c\vec{k}} - \omega_{v\vec{k}})^2 - \omega^2]^2 + (\Gamma\omega)^2} \quad (5)$$

and

$$\epsilon_2(\hat{e};\omega) = \omega_p^2 \sum_{c,v} \sum_{\vec{k}} f_{v\vec{k}}^{c\vec{k}}(\hat{e}) \frac{\Gamma\omega}{[(\omega_{c\vec{k}} - \omega_{v\vec{k}})^2 - \omega^2]^2 + (\Gamma\omega)^2} \quad (6)$$

For computational reasons, we have included only vertical band-to-band transitions in the implementation of eqs 5 and 6, thus disregarding the intra-band electronic transitions that give an important contribution to the low-frequency spectral region of the metallic systems. A simplified way of taking into account this contribution is through the Drude theory of metals, which suggests to complement the real and imaginary parts of the dielectric function, calculated including only inter-band transitions, as follows:

$$\bar{\epsilon}_1(\hat{e};\omega) = \epsilon_1(\hat{e};\omega) - \omega_p^2 \frac{f_D}{\omega^2 + \gamma^2}$$

$$\bar{\epsilon}_2(\hat{e};\omega) = \epsilon_2(\hat{e};\omega) + \omega_p^2 \frac{f_D\,\gamma}{\omega(\omega^2 + \gamma^2)} \quad (7)$$

where f_D and γ represent phenomenological parameters for the free carriers of the metallic system. In fact, we have used these parameters to best fit the frequency dependence of the real part of the dielectric constant measured on PANI-CSA polymers.[47]

We point out that this way of including the effects of the intra-band transitions represents an a posteriori, phenomenological correction of the ab initio dielectric function. Therefore, it does not ensure the rigorous fulfilment either of the dispersion relations or of the sum rule. In the case of the ES-II polymer, we have found that our ab initio calculations, which take into account only inter-band transitions, give $\Sigma_{c,v}\Sigma_{\vec{k}} f_{v\vec{k}}^{c\vec{k}} = 0.885$; the best fit value obtained for the strength of the Drude oscillator is $f_D = 0.014$. Adding these oscillator strengths, we obtain a 90% fulfillment of the corresponding sum rule. Furthermore, our best fit value for the Drude damping parameter is $\hbar\gamma = 0.55$ eV. This value, if used to estimate the dc conductivity of the polymer, gives $\sigma(\omega{=}0) = \omega_p^2(f_D\gamma/4\pi) \simeq 1187$ S cm^{-1}, in good agreement with the experimental value, measured at $T = 300$ K on PANI-CSA polymers,[47] that is, $\sigma(\omega{=}0) \simeq 1100$ S cm^{-1}.

The optical properties calculated in this paper are the following:

(a) real (+) and imaginary (−) parts of the complex refractive index

$$n_{\pm}(\hat{e};\omega) = \sqrt{\frac{1}{2}\sqrt{\epsilon_1(\hat{e};\omega)^2 + \epsilon_2(\hat{e};\omega)^2} \pm \frac{1}{2}\epsilon_1(\hat{e};\omega)} \quad (8)$$

(b) optical absorption spectrum

$$\alpha(\hat{e};\omega) = \frac{\omega}{c n_+(\hat{e};\omega)} \epsilon_2(\hat{e};\omega) = \frac{2\omega}{c} n_-(\hat{e};\omega) \quad (9)$$

(c) optical conductivity

$$\sigma(\hat{e};\omega) = \frac{\omega}{4\pi} \epsilon_2(\hat{e};\omega) \quad (10)$$

(d) reflectance

$$R(\hat{e};\omega) = \frac{[n_+(\hat{e};\omega) - 1]^2 + n_-(\hat{e};\omega)^2}{[n_+(\hat{e};\omega) + 1]^2 + n_-(\hat{e};\omega)^2} \quad (11)$$

3. Results

For the ES-II polymer, we have used a *Pc*2*a* orthorhombic cell (lattice parameter: $a = 7.1$ Å, $b = 7.9$ Å, $c = 20.84$ Å) with two strands of polymer chains inside, each one with four ($-C_6H_4NH-$) groups and two adjacent chlorine atoms in polaronic positions (see ref 49). The structural and electronic results obtained for ES-II[49] show that each polymer chain consists of a repeat unit $[(1S)^{\bullet+}(Cl)^-]_n$, and the two strands of polymer chains in the cell are mutually shifted by one complete ring along the chain backbone. Thus, we have consistently reduced the *c*-axis of our simulation cell by a factor two ($c = 10.42$ Å), including two strands of polymer chains with repeat unit $[(1S)^{\bullet+}(Cl)^-]_n$ and geometrical parameters taken from Table 1 and 2 of ref 49.

For the EB-II polymer, we have used the *Pbcn* orthorhombic cell defined in ref 52 (lattice parameter: $a = 7.80$ Å, $b = 5.75$ Å, $c = 20.25$ Å) with two strands of polymer chains inside, each one with three phenilene rings, one quinoid ring, two amine and two imine nitrogen atoms, and with geometrical parameters taken from Table 1 and 2 of ref 52.

3.1. Optical Absorption Spectra. In Figure 1a, we plot the absorption coefficient $\alpha(\hat{c};\omega)$ calculated with the ab initio components $\epsilon_{1,2}(\hat{c};\omega)$ of the dielectric function. In eqs 5 and 6, we have used $\hbar\Gamma = 0.3$ eV and a linearly polarized light parallel to the *c*-axis of the cell, i.e., to the direction of the chain backbone. Note that $\alpha(\hat{c};\omega)$ is the largest component of the absorption coefficient $\alpha(\hat{e};\omega)$; thus, even plotting the average value of the three components of $\alpha(\hat{e};\omega)$, the resulting spectrum mantains almost the same profile. In Figure 1a, we have also plotted the absorption spectrum calculated for the ES-II polymer without counterions, i.e., with two strands of chains with repeat unit $[(1S)^{\bullet+}]_n$ inside the same crystalline cell. Comparing the two plots of Figure 1a, we see that the spectral contribution of the counterions is negligible, in agreement with the fact that absorption spectra recorded on samples with different counterions have almost identical profiles.

In Figure 1b,c, we plot the energy-band structure of the system without and with counterions, respectively, and in Figure 1d, e, we plot the corresponding densities of states (DOS). Comparing these figures, we see that the only contributions of the Cl^- counterions are the flat bands due to their 3p levels in the region between 1 and 2 eV below the Fermi level. (Note

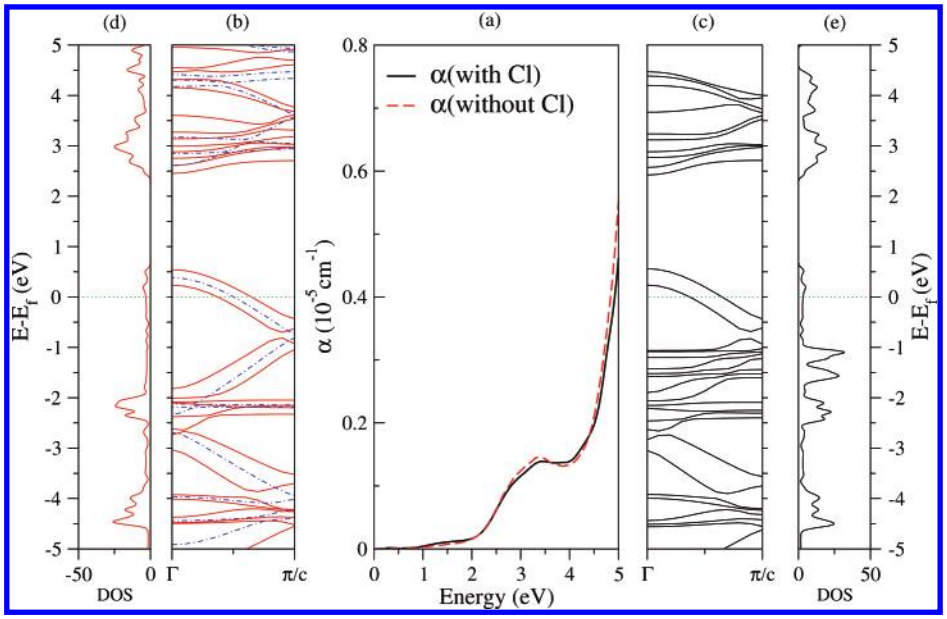

Figure 1. (a) Absorption coefficient, $\alpha(\hat{c};E)$, for a linearly polarized light along the direction of the polymer chains. The dashed line corresponds to the absorption spectrum of the system without counterions. (b, c) Energy-band structures, measured from the Fermi energy and plotted along the *c*-axis of the reciprocal space, of the ES-II polymer without counterions (b) and with counterions in polaronic positions (c); the dashed-dot lines in (b) are the energy bands of an isolated polymer chain of ES-II without counterions. (d, e) Total densities of states (DOS) corresponding to the energy-band structures shown in (b, c), respectively.

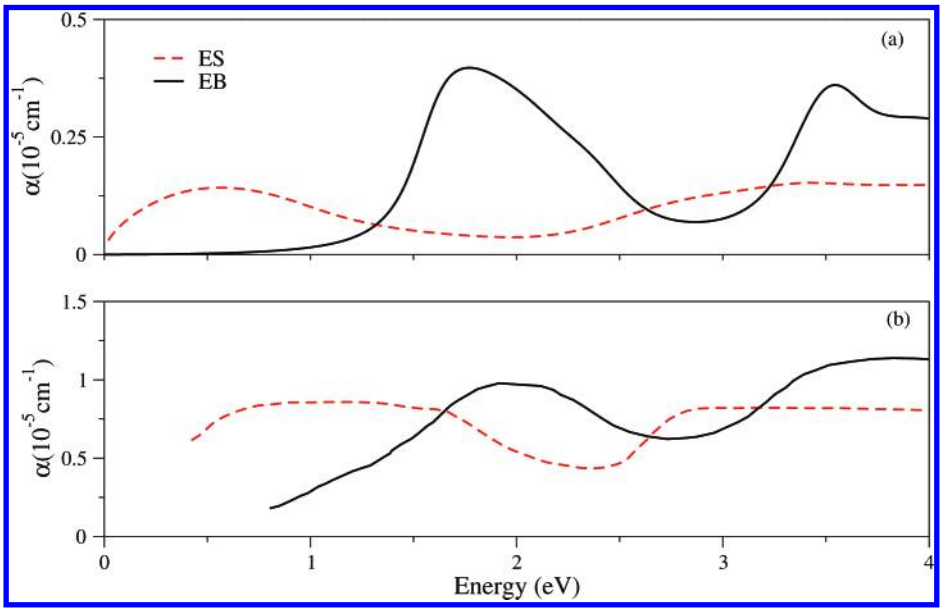

Figure 2. Comparison between calculated (a) and experimental (b) absorption spectra of ES and EB polymers. Figure 2b has been adapted from Figure 3 of ref 20.

that the Fermi energy has been calculated by integrating the DOS to the proper number of electrons.) The energy-band structure with the characteristic doubling of the bands makes evident the presence of two interacting chains in the unit cell. For comparison, in Figure 1b, we have plotted also the band structure of an isolated chain of the polymer without counterions. We observe that, considering only vertical transitions, Figure 1b predicts the onsets of an intra-chain absorption band around 1 eV and of an inter-chain absorption band around 1.5 eV. Looking, however, to the absorption spectrum of Figure 1a, obtained with the explicit calculation of the transition matrix elements in $\epsilon(\hat{c};\omega)$, we see that the intensity of the transitions below 2 eV is quite low; the absorption spectrum, indeed, has its first relevant peak around 3.5 eV, where both intra- and inter-chain transitions from partially and fully occupied bands give their contributions.

In Figure 2, we compare an experimental absorption spectrum[20] of ES, recorded on polyaniline film spin-cast from sulfuric acid solution and subsequently equilibrated with aqueous HCl solution (pH = 0.15), with the "theoretical" absorption spectrum calculated using the dielectric function $\bar{\epsilon}(\hat{c};\omega)$ that includes the Drude term for intra-band transitions. We see that the "theoretical" spectrum shows, now, a broad absorption region below 1.5 eV, slightly red-shifted with respect to the corresponding region in the experimental spectra (see also Figure 1b of ref 32 and Figure 4a of ref 18). Nevertheless, the global profile of the theoretical spectrum follows quite satisfactorily the experimental one.

In Figure 2, we also compare the absorption spectrum measured on film of an EB polymer[20] with the theoretical absorption spectrum calculated for the EB-II polymer of ref 52. Because EB is a semiconductor (direct gap $\sim$ 1.4 eV), we have

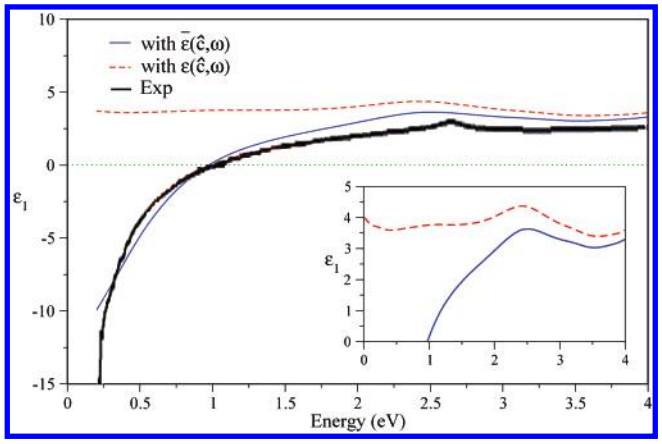

Figure 3. Measured spectrum of the real part of the dielectric function of PANI-CSA salts,[47] compared with the spectra calculated with and without the Drude term. The inset shows details of the calculated curves in the frequency region of interest.

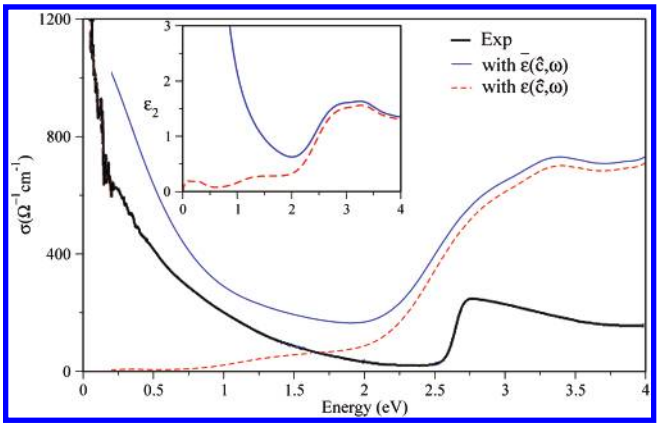

Figure 4. Measured spectrum of the optical conductivity of PANI-CSA salts[47] compared with $\sigma(\hat{c};\omega)$ calculated with and without the Drude term. The inset shows the ω-dependence of $\epsilon_2(\hat{c};\omega)$ and $\bar{\epsilon}_2(\hat{c};\omega)$ in the region of interest.

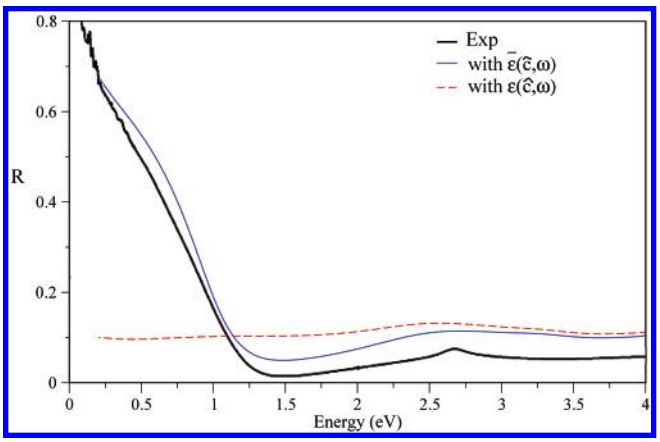

Figure 5. Measured spectrum of the reflectance of PANI-CSA salts[47] compared with $R(\hat{c};\omega)$ calculated with and without the Drude term.

used the dielectric function $\epsilon(\hat{c};\omega)$ without a Drude correction, and we have applied a scissor operator of 0.8 eV, i.e., a *k*-independent self-energy correction that shifts rigidly the conduction bands to enlarge the band gap underestimated in the DFT calculations.[62] We see that the theoretical spectrum of EB reproduces quite satisfactorily the two characteristic peaks around 2 and 3.5 eV. The first one is ascribed to a charge-transfer transition associated with excitation from benzenoid to quinoid rings and the latter to a $\pi \rightarrow \pi^*$ band gap absorption.[32,63] Upon protonation of EB to give ES, the first peak vanishes and two absorption regions appear centered around 1 and 3 eV, respectively.

We observe that the spectral profiles of the absorption spectra calculated for EB-II and ES-II are in substantial agreement with the experimental ones, even if the ratio of the ES/EB intensities is slightly underestimated in the theoretical spectrum.

3.2. Dielectric Function, Optical Conductivity, and Reflectance. In this section, we present the $\epsilon_1(\hat{c};\omega)$, $\sigma(\hat{c};\omega)$, and $R(\hat{c};\omega)$ spectra calculated for the ES-II crystalline polymer of ref 49, and we compare these spectra with those recorded on PANI-CSA salts[47] prepared from SSDP samples of PANI-EB. The comparison is based on the assumption that lattice structure and polymer chains of PANI-CSA are not too different from those of ES-II,[49] and the specific contribution of the counterions to the optical spectra of these polymers can be neglected. We point out also that our comparison with the experimental spectra does not include the ω-region below 0.2 eV, where phonon contributions are dominant.

In Figure 3, we compare the measured and calculated spectra of the real part of the dielectric function; we have plotted separately $\epsilon_1(\hat{c};\omega)$ and $\bar{\epsilon}_1(\hat{c};\omega)$ to make evident the contributions of the inter- and intra-band transitions. An appropriate choice of the f_D and γ parameters in eq 7 makes $\bar{\epsilon}_1(\hat{c};\omega)$ to cross zero around $\hbar\omega \sim 1$ eV, as in the experiment, and to remain negative down to $\hbar\omega \sim 0.2$ eV (the limit value for our comparison with the experiment). We see that the characteristic bump around 2.7 eV in the experimental spectrum is slightly red-shifted by the ab initio component $\epsilon_1(\hat{c};\omega)$ of the dielectric function, but the overall agreement between calculated and measured spectra is remarkable.

In Figure 4, we compare the measured spectrum of the optical conductivity[47] with the spectra calculated with and without the Drude term. In this case, the "theoretical" curve overestimates appreciably the experimental one and gives only a qualitative picture of the spectral profile. To improve the quality of the calculated spectrum, one should probably include a larger number of *k*-points in the calculation of the dielectric function, a request that is beyond our actual computational capabilities.

Finally, in Figure 5, we compare the measured spectrum of reflectance[47] with the spectra calculated with and without the Drude term. We see, again, a remarkable agreement between theory and experiment: the "theoretical" curve reproduces the characteristic minimum around 1.4 eV, ascribed to the free-carrier plasma resonance typical of a metal,[47] and the bump in the region around 2.7 eV due to inter-band transitions.

4. Conclusions

We have shown the possibility of calculating optical spectra of good quality for crystalline polymers obtained by chemical protonation of conjugated polymers. We have used KS-wavefunctions and energies implemented in the quantum-mechanical expression of the macroscopic transverse dielectric function in the framework of the band theory without the electron−hole interaction. To take into account also contributions of the intra-band transitions, we have added, to the dielectric function calculated ab initio, a Drude-like term appropriate for metallic systems.

The calculated spectra are in remarkable agreement with the experiment and allow one to identify contributions of inter- and the intra-band electronic transitions to the optical properties of these polymers. The analysis of the single-particle energy bands also makes evident the influence of the crystalline structure of the polymer: because of the specific crystal symmetry with two

chains per unit cell, all bands are doubled and interchain transitions give a relevant contribution to the optical spectra. This fact confirms the need of a fully 3D approach to the study of these polymeric systems.

We have also shown that absorption spectrum and other important optical properties of PANI salts obtained from chemical doping of conjugated polymers are not directly influenced by the type of counterions produced in the acidification process. The crystalline structure of ES-II with Cl^- counterions in polaronic positions represents indeed a structure appropriate also for calculating optical properties of other PANI salts.

Acknowledgment. We thank Giuseppe Grosso for helpful discussions and suggestions. This work has been supported by MURST-PRIN 2004. We acknowledge the allocation of computer resources from CNR-INFM "Parallel Computing Initiatives" and Cineca Supercomputing Center.

References and Notes

(1) Shirakawa, H.; Louis, E. J.; MacDiarmid, A. G.; Chiang, C. K.; Heeger, A. J. *J. Chem. Commun*. **1977**, 578.

(2) Chiang, C. K.; Fincher, C. R.; Park, Y. W.; Heeger, A. J.; Shirakawa, H.; Louis, E. J.; Gau, S. C.; MacDiarmid, A. G. *Phys. Rev. Lett.* **1977**, *39*, 1098.

(3) Ranby, B. In *Conjugated Polymers and Related Materials: The Interconnection of Chemical and Electronic Structures*; Salaneck, W. R., Lundström, I., Ranby, B., Eds.; Oxford University Press: Oxford, U.K., **1993**; Chapter 3.

(4) Heeger, A. J. *J. Phys. Chem. B* **2001**, *105*, 8475.

(5) *Organic Electronic Materials: Conjugated Polymers and Low Molecular Weight Organic Solids*; Farchioni, R., Grosso, G., Eds.; Springer: Berlin, 2001; Vol. 41.

(6) *Conjugated Polymers: The Novel Science and Technology of Highly Conducting and Nonlinear Optically Active Materials*; Brédas, J. L., Silbery, R., Eds.; Kluwer: Dordrecht, The Netherlands, 1991.

(7) *Science and Applications of Conducting Polymers*; Salaneck, W. R., Clark, D. T., Samuelsen, E. J., Eds.; Adam Hilger: Bristol, U.K., 1991.

(8) *Polymers and Other Advanced Materials. Emerging Technologies and Business Opportunities*; Prasad, P. N.; Mark, J. E.; Fai, T. J., Eds; Plenum: London, 1995.

(9) *Electrical, Optical, and Magnetic Properties of Organic Solid State Materials, III*; Jean, A. K.-Y., Lee, C. Y. -C., Dalton, L. R., Rubner, M. F., Wnek, G. E., Chang, L. Y., Eds.; *Mater. Res. Soc. Symp. Proc. No. 179*; Material Research Society: Pittsburg, PA, 1996.

(10) *Electrical and Optical Polymers*; Wnek, G., Trantolo, D. J., Cooper, T. M., Gresser J. D., Eds.; Marcel Dekker: New York, 1997.

(11) Liu, W.; Kuwer, J.; Tripathy, S.; Senecal, K. J.; Samuelson, L. *J. Am. Chem. Soc.* **1999**, *121*, 71.

(12) Pei, Q.; Yu, G.; Zhang, C.; Yang, Y.; Heeger, A. J. *Science* **1995**, *269*, 1086.

(13) Somani, P. R.; Radhakrishnan, S. *Mater. Chem. Phys.* **2002**, *77*, 117.

(14) Nigrey, P. J.; MacDiarmid, A. G.; Heeger, A. J. *J. Chem. Commun.* **1979**, 96, 594.

(15) Salaneck, W. R.; Lundstrom, I.; Huang, W. S.; MacDiarmid, A. G. *Synth. Met.* **1986**, *13*, 291.

(16) Chiang, J. C.; MacDiarmid, A. G. *Synth. Met.* **1986**, *13*, 193.

(17) MacDiarmid, A. G.; Chiang, J. C.; Richter, A. F.; Epstein, A. J. *Synth. Met.* **1987**, *18*, 285.

(18) Epstein, A. J.; Ginder, J. M.; Zuo, F.; Bigelow, R. W.; Woo, H.-S.; Tanner, D. B.; Richter, A. F.; Huang, W.-S.; MacDiarmid, A. G. *Synth. Met.* **1987**, *18*, 303.

(19) MacDiarmid, A. G.; Epstein, A. J. In *Electrical, Optical and Magnetic Properties of Organic Solid State Materials*; Chang, L. Y., Cowan, D. O., Chaikin, P. M., Eds.; *Mater. Res. Soc. Symp. Proc. No. 173*; Material Research Society: Pittsburg, PA, 1990; p 283.

(20) Cao, Y.; Smith, P.; Heeger, A. J. *Synth. Met.* **1989**, *32*, 263.

(21) Cao, Y.; Smith, P.; Heeger, A. J. *Synth. Met.* **1992**, *48*, 91.

(22) Yang, C. Y.; Cao, Y.; Smith, P.; Heeger, A. J. *Synth. Met.* **1992**, *53*, 293.

(23) Ginder, J. M.; Richter, A. F.; MacDiarmid, A. G.; Epstein, A. J. *Solid State Commun.* **1987**, *63*, 97.

(24) Józefowicz, M. E.; Laversanne, R.; Javadi, H. H. S.; Epstein, A. J.; Pouget, J.; Tang, X.; MacDiarmid, A. G. *Phys. Rev. B* **1989**, *39*, R12958.

(25) Pouget, J. P.; Józefowicz, M. E.; Epstein, A. J.; Tang, X.; MacDiarmid, A. G. *Macromolecules* **1991**, *24*, 779.

(26) Laridijani, M.; Pouget, J. P.; Scherr, E. M.; MacDiarmid, A. G.; Józefowicz, M. E.; Epstein, A. J. *Macromolecules* **1992**, *25*, 4106.

(27) Winokur, M. J.; Mattes, B. R. *Macromolecules* **1998**, *31*, 8183.

(28) Colomban, Ph.; Folch, S.; Gruger, A. *Macromolecules* **1999**, *32*, 3080.

(29) Mazarolles, M.; Folch, S.; Colomban, Ph. *Macromolecules* **1999**, *32*, 8504.

(30) MacDiarmid, A. G.; Epstein, A. J. *Conjugated Polymeric Materials: Opportunities in Electronics, Optical Electronics and Molecular Electronics*; Brédas, J. L., Chance, R. R., Eds.; Kluwer Academic Publishers: Dordrecht, The Netherlands, 1990; p 53.

(31) Wudl, F.; Angus, R. O.; Lu, F. L.; Allemand, P. M.; Vachon, D. J.; Nowak, M.; Liu, Z. X.; Heeger, A. J. *J. Am. Chem. Soc.* **1987**, *109*, 3677.

(32) Roe, M. G.; Ginder, J. M.; Wigen, P. E.; Epstein, A. J.; Angelopoulos, M.; MacDiarmid, A. G. *Phys. Rev. Lett.* **1988**, *60*, 2789.

(33) Folch, S.; Regis, A.; Gruger, A.; Colomban, Ph. *Synth. Met.* **2000**, *110*, 219.

(34) Boudreaux, D. S.; Chance, R. R.; Wolf, J. F.; Shacklette, L. W.; Brédas, J. L.; Themans, B.; Andre, J. M.; Silbey, R. *J. Chem. Phys.* **1986**, *85*, 4584.

(35) Stafström, S.; Brédas, J. L.; Epstein, A. J.; Woo, H. S.; Tanner, D. B.; Huang, W. S.; MacDiarmid, A. G. *Phys. Rev. Lett.* **1987**, *59*, 1464.

(36) Libert, J.; Brédas, J. L.; Epstein, A. J. *Phys. Rev. B* **1995**, *51*, 5711.

(37) Varela-Alvarez, A.; Sordo, J. A.; Scuseria, G. E. *J. Am. Chem. Soc.* **2005**, *127*, 11318.

(38) Wang, Z. H.; Li, J.; Scherr, E. M.; MacDiarmid, A. G.; Epstein, A. J. *Phys. Rev. Lett.* **1991**, *66*, 1745.

(39) Wang, Z. H.; Scherr, E. M.; MacDiarmid, A. G.; Epstein, A. J. *Phys. Rev. B* **1992**, *45*, 4190.

(40) Reghu, M.; Cao, Y.; Moses, D.; Heeger, A. J. *Phys. Rev. B* **1993**, *47*, 1758.

(41) Lee, K.; Heeger, A. J.; Cao, Y. *Phys. Rev. B* **1993**, *48*, 14884.

(42) Joo, J.; Pouget, J.; Oh, E. J.; MacDiarmid, A. G.; Epstein, A. *J. Phys. Rev. B* **1998**, *57*, 9567.

(43) Tzamalis, G.; Zaidi, N. A.; Homes, C. C.; Monkman, A. P. *Phys. Rev. B* **2002**, *66*, 085202.

(44) Heeger, A. J. *Phys. Scr.* **2002**, *T102*, 30.

(45) Lee, K. In *Encyclopedia of Nanoscience and Nanotechnology*; Naiwa, H. S., Ed.; American Scientific Publishers: San Diego, 2004; Vol. 5; pp 537−549.

(46) Lee, K.; Heeger, A. J. *Synth. Met.* **2002**, *128*, 279.

(47) Lee, K.; Cho, S.; Park, S. H.; Heeger, A. J.; Lee, C.-W.; Lee, S.-H. *Nature* **2006**, *441*, 65.

(48) Lee, S.-H.; Lee, D.-H.; Lee, K.; Lee, C.-W. *Adv. Funct. Mater.* **2005**, *15*, 1495.

(49) Cavazzoni, C.; Colle, R.; Farchioni, R.; Grosso, G. *Phys. Rev. B* **2006**, *74*, 033103.

(50) Car, R.; Parrinello, M. *Phys. Rev. Lett.* **1985**, *55*, 2471.

(51) For a recent review, see Marx, D.; Hutter, J. In *Modern Methods and Algorithms of Quantum Chemistry*; Grotendorst, J., Ed.; NIC: FZ Jülich, Germany, 2000.

(52) Cavazzoni, C.; Colle, R.; Farchioni, R.; Grosso, G. *Phys. Rev. B* **2004**, *69*, 115213.

(53) Rohlfing, M.; Louie, S. G. *Phys. Rev. B* **2000**, *62*, 4927.

(54) Ruini A.; Caldas, M. J.; Bussi G.; Molinari E. *Phys. Rev. Lett.* **2002**, *88*, 206403, and references therein.

(55) Hummer, K.; Ambrosch-Draxl, C. *Phys. Rev. B* **2005**, *72*, 205205.

(56) Ambrosch-Draxl, C.; Hummer K.; Sagmeister S.; Puscnig P. *Chem. Phys.* **2006**, *325*, 3, and references therein.

(57) See http://www.quantum-espresso.org.

(58) Troullier, N.; Martins, J. L. *Phys. Rev. B* **1991**, *43*, 1993.

(59) Becke, A. D. *Phys. Rev. A* **1988**, *38*, 3098.

(60) Lee, C.; Yag, W.; Parr, R. G. *Phys. Rev. B* **1988**, *37*, 785.

(61) Baroni, S.; Resta, R. *Phys. Rev. B* **1986**, *33*, 7017.

(62) Godby, R. W.; Schlüter, M.; Sham, L. J. *Phys. Rev. B* **1988**, *37*, 10159.

(63) McCall, R. P.; Ginder, J. M.; Leng, J. M.; Ye, H. J.; Manohar, S. K.; Master, J. G.; Asturias, G. E.; MacDiarmid, A. G.; Epstein, A. J. *Phys. Rev. B* **1990**, *41*, 5202.